TLR2 promotes traumatic deep venous thrombosis of the lower extremity following femoral fracture by activating the NF-κB/COX-2 signaling pathway in rats

TIANTING GUO[1*], LIJIAO XIONG[2,3*], JUNBIN XIE[1], JIWEI ZENG[1], ZHIHUA HUANG[4], MENGTING YAO[4], XIAOAN ZHANG[1] and JIANWEN MO[3]

[1]Department of Orthopedics, Ganzhou Hospital of Guangdong Provincial People's Hospital, Ganzhou Municipal Hospital, Ganzhou, Jiangxi 341000, P.R. China; [2]Department of Geriatrics, The First Affiliated Hospital (Shenzhen People's Hospital), Southern University of Science and Technology, Shenzhen, Guangdong 518055, P.R. China; [3]Department of Geriatrics, The First Affiliated Hospital of Gannan Medical University, Ganzhou, Jiangxi 341000, P.R. China; [4]Key Laboratory of Prevention and Treatment of Cardiovascular and Cerebrovascular Diseases of Ministry of Education, Gannan Medical University, Ganzhou, Jiangxi 341000, P.R. China

Received November 24, 2023; Accepted June 28, 2024

DOI: 10.3892/etm.2024.12725

Abstract. Endothelial cells (ECs) are crucial for maintaining the integrity of blood vessel walls and reducing thrombosis. Deep venous thrombosis (DVT) is a common thrombotic disease and its diagnosis and treatment remain at the stage of coagulation function examination and post-onset treatment. Thus, identifying the pathogenesis of DVT is important. The present study investigated the significance of the Toll-like receptor 2 (TLR2)/nuclear factor kappa B (NF-κB)/cyclooxygenase-2 (COX-2) signaling pathway in a human umbilical vein EC (HUVECs) oxygen glucose deprivation (OGD) model and femoral fractures were induced in anesthetized rats using a quantifiable impact device delivering 5 J of energy to each side of the proximal outer thigh, followed by external fixation with a hip spica cast to create a traumatic deep venous thrombosis (TDVT) animal model. Rats were subjected to quantitative impact fixation to establish a TDVT model. The rats were treated with a TLR2 agonist (Pam3CSK4) and a TLR2 inhibitor (C29) via intraperitoneal injection and thrombus formation was examined. HUVECs were subjected to OGD and treated with Pam3CSK4 or C29 and cell viability and apoptosis were assessed. Western blotting, immunofluorescence and reverse transcription-quantitative PCR were used to examine the inflammatory responses and signaling pathways. *In vivo* experiments showed that Pam3CSK4 promoted thrombus formation and increased the mRNA and protein expression of NF-κB, COX-2, Tissue factor (TF), IL-6 and P-selectin compared with the model and C29 groups. *In vitro* experiments showed that Pam3CSK4 treatment resulted in a higher number of apoptotic cells than C29 treatment and that it increased the levels of NF-κB, COX-2, IL-6 and P-selectin, whereas C29 decreased them. Thus, TLR2 promotes the inflammatory response in EC through the NF-κB/COX-2 signaling pathway, which may lead to EC apoptosis and the occurrence of TDVT.

Correspondence to: Dr Jianwen Mo, The First Affiliated Hospital of Gannan Medical University, 23 Qingnian Road, Ganzhou, Jiangxi 341000, P.R. China
E-mail: mjw1997@126.com

Dr Xiaoan Zhang, Department of Orthopedics, Ganzhou Hospital of Guangdong Provincial People's Hospital, Ganzhou Municipal Hospital, 49 Dagong Road, Ganzhou, Jiangxi 341000, P.R. China
E-mail: zhangxa1972@126.com

*Contributed equally

Abbreviations: COX-2, cyclooxygenase-2; DVT, deep vein thrombosis; HUVEC, human umbilical vein endothelial cell; NF-κB, nuclear factor kappa B; OGD, oxygen glucose deprivation; TDVT, traumatic deep vein thrombosis; TLR2, Toll-like receptor 2

Key words: Toll-like receptor 2, traumatic deep vein thrombosis, cyclooxygenase-2, signaling pathway

Introduction

Deep venous thrombosis (DVT) is a common thrombotic disease. According to previous reports, the incidence of DVT in trauma patients without prophylaxis can be as high as 80% (1). Orthopedic trauma patients are at a high risk for DVT owing to various risk factors and the incidence of venous thromboembolism in orthopedic trauma patients ranges from 20.81-43.4% (2-5). Although prophylactic medication can reduce the rate of DVT, the morbidity and mortality rates of pulmonary embolism caused by DVT remain high. Studies have shown that ~6% of patients with DVT and 12% of patients with pulmonary embolism succumb within 1 month of diagnosis, seriously endangering the life and health of patients (4). The current mechanisms of interaction between certain therapeutic anticoagulants are diverse and monitoring changes in coagulation factors is required in some cases during the use of these medications (6). Therefore, further exploration

of the DVT pathogenesis is required to develop new treatment strategies (7).

Endothelial cell (EC) damage is a key factor in TDVT. When the endothelium is traumatized by fractures, trauma, surgery, or other external factors, an inflammatory response and EC apoptosis can occur. Simultaneously, it can promote the aggregation of platelets and white blood cells as well as the activation of the coagulation system, leading to thrombosis (8). During this process, a number of cells and molecules, including monocytes, T cells, platelets and coagulation factors, interact with each other. Excessive expression of cytokines, such as interleukin IL-6, cyclooxygenase-2 (COX-2) and tumor necrosis factor-α (TNF-α), can lead to EC damage and death (9,10).

Toll-like receptor 2 (TLR2) is a receptor that recognizes microbial components and plays critical roles in infection and inflammation (11). Cluster of differentiation 14 (CD14) is an auxiliary protein of TLR2 that can bind to TLR2 to activate the TLR2 signaling pathway (12). In ECs, TLR2 and CD14 regulate inflammatory responses through mutual interactions (13). When pathogens or other stimuli enter the body, they bind to TLR2 and activate the TLR2 signaling pathway. The involvement of TLR2 leads to the activation of the nuclear factor-kappa B (NF-κB) pathway, increasing gene expression and the release of proinflammatory mediators, such as IL-1β and TNF-α, resulting in local inflammation (13,14). The expression and activation of TLR2 have been shown to regulate the function of a number of cell types such as dendritic cells, monocytes and neutrophils (14). In addition, TLR2 and CD14 can regulate the apoptosis and proliferation of ECs, which influence the integrity and stability of the endothelial barrier (15). Previous studies showed that TLR2 expression increased in TDVT samples (16,17). The present study aimed to further clarify the regulatory mechanism of the TLR2/NF-κB/COX-2 signaling pathway in TDVT.

Materials and methods

Animals. Specific pathogen-free (SPF) Sprague-Dawley (SD) experimental rats were purchased from Sleek Venture Experimental Animals Co., Ltd. [license number: SCXK (Xiang) 2019-0004]. The experimental unit used the license number SYXK (Gan) 2018-0004. A total of 30 male SPF SD rats (weighing 200-220 g, 6-to 8-week-old) were housed at the Laboratory Animal Center of Gannan Medical University (Ganzhou, China) under standard conditions of temperature (20-25˚C), humidity (50-60%) and lighting (12-h light/dark cycle), with free access to food and water. The rats were allowed to adapt for 3-5 days before the experiment. All animal experiments were conducted in the animal laboratory of the Laboratory Animal Center of Gannan Medical University and were approved by the Ethics Committee of Gannan Medical University (approval no. LLSC-2022110701). All animal procedures were performed following the guidelines of the Council on Animal Care (18). The research complied with the Five Freedoms (freedom from hunger and thirst, freedom from discomfort, freedom from pain, injury and disease, freedom to express normal behavior, freedom from fear and distress) and the 3R principles (Replacement, Reduction and Refinement) for experimental animals was observed. The present study strictly followed the regulations and guidelines set by the ethics committee to ensure that the welfare and rights of the animals were respected and protected.

On the day of the experiments, the animals were anesthetized with intravenous pentobarbital sodium (30 mg/kg). The rats were anesthetized and maintained under anesthesia throughout the experiment. At the end of the experiment, deep anesthesia was induced for sample collection, followed by euthanasia via intraperitoneal injection of 3% pentobarbital sodium (100 mg/kg) to ensure a painless and humane procedure. Experimental procedures and handling were conducted by trained professionals who ensured the scientific validity and reliability of the experiment.

TDVT model. The TDVT model, widely used in the present study, was established as follows: 28 male SPF SD rats weighing 200-220 g were randomly divided into sham operation group, model group, C29 group and Pam3CSK4 group. Except for the sham operation group, all SD rats were placed in the supine position and anesthetized with 3% sodium pentobarbital solution at a dose of 1 mg/kg via intravenous injection. Following anesthesia induction, a self-made traumatic quantifiable impact device (19) was used to deliver an instantaneous energy of 5 J striking each side of the proximal outer thigh of the rats once (1 cm below the greater trochanter) (19). Fractures of the femur were confirmed by bone scraping sensation or abnormal activity and confirmed by X-ray imaging. A window was created on the surface of the plaster in the superficial femoral vein area of the inner thigh on both sides to observe the formation of thrombus. After modeling, the experimental rats were allowed free access to food and water without the use of hemostatic agents or antibiotics. At 0, 24, 48 and 96 h post-modeling, rats in the sham operation and model groups were intraperitoneally injected with an equal volume of physiological saline; the C29 group received 5 mg/kg C29 (cat. no. HY-100461; MedChemExpress) (20) and the Pan3CSK4 group received 1 mg/kg Pam3CSK4 (InvivoGen) (21,22), Based on the results of preliminary experiments, 5 mg/kg of C29 and 1 mg/kg of PAM3CSK4 were selected to achieve a balance between the mortality rate of experimental animals and experimental effectiveness.

Collection and measurement of the venous thrombus. The rats were anesthetized via intraperitoneal injection of 3% pentobarbital sodium solution (30 mg/kg) and routine disinfection. At 24 h after the last administration, deep anesthesia was induced for sample collection, followed by euthanasia via intraperitoneal injection of 3% pentobarbital sodium (100 mg/kg). The size, length and weight of deep vein thrombosis and thrombus formation rate were measured.

Cell culture and grouping. Human umbilical vein EC (HUVECs; immortalized human umbilical vein EC Line Certificate of STR Analysis:FH1122, STR 20170721-05) were purchased from Shanghai Fuheng Biology Co, Ltd. and cultured in RPMI-1640 (cat. no. 22400089; Gibco; Thermo Fisher Scientific, Inc.) supplemented with 10% fetal bovine serum (cat. no. 10099141; Gibco; Thermo Fisher Scientific, Inc.) and 1% penicillin/streptomycin (cat. no. P1400-100;

Table I. Sequences of primers used for RT-PCR analysis.

Gene	Primer	Sequence (5'-3')	PCR Products
GAPDH	Forward	TCAAGAAGGTGGTGAAGCAGG	115 bp
	Reverse	TCAAAGGTGGAGGAGTGGGT	
TLR2	Forward	TGTGAAGAGTGAGTGGTGCA	208 bp
	Reverse	TACCCAAAATCCTTCCCGCT	
IL-6	Forward	AGGAGACTTGCCTGGTGAAA	180 bp
	Reverse	CAGGGGTGGTTATTGCATCT	
COX-2	Forward	CTCCTGTGCCTGATGATTGC	169 bp
	Reverse	AACTGATGCGTGAAGTGCTG	
P-selectin	Forward	TGCCAGAATCGCTACACAGA	181 bp
	Reverse	TATCAGCCCAGTTCTCAGCC	
TF	Forward	ACCCCAACTGGTGATGAAAG	200 bp
	Reverse	GAATGGCTGTTGTTGTAAATG	

TLR2, Toll-like receptor 2; COX-2, cyclooxygenase-2; TF, tissue factor.

Beijing Solarbio Science & Technology Co., Ltd.) in a 5% CO_2 incubator at 37˚C. At the logarithmic growth stage, the cells were divided into control, oxygen-glucose deprivation (OGD) model (model), Pam3CSK4 and C29 groups. All the cells were subjected to OGD, with the exception of those in the control group. The HUVECs were treated with Pam3CSK4 (1 μmol/l) or C29 (1 μmol/l) for 1 h before OGD (23). Meanwhile, an equal volume of RMPI-1640 was added to the control and OGD groups. To induce OGD, the cells were rinsed and incubated in glucose-free RPMI 1640 (cat. no. 11879020; Gibco; Thermo Fisher Scientific, Inc.) saturated with 95% N_2 and 5% CO_2 for 6 h. The cells were then rinsed and maintained under normal conditions for 24 h.

Cell counting kit 8 (CCK8). HUVECs at the logarithmic growth stage were seeded into 96-well plates (3,000 cells/well) and treated with Pam3CSK4 (0.1, 1.0 and 10 μmol/l) or C29 (0.1, 1.0 and 10 μmol/l) for 24, 48 and 72 h. CCK8 proliferation assay was performed using a CCK8 Kit (cat. no. CA1210; Beijing Solarbio Science & Technology Co., Ltd.) according to the manufacturer's instructions. Each well was treated with 10 μl of CCK8 for 4 h and the absorbance was measured at 450 nm using a microplate reader (VLBLATD2 Multifunctional enzyme marker; Thermo Fisher Scientific, Inc.). Each group had six wells and the experiment was repeated thrice.

Annexin V-FITC/PI flow cytometry. HUVECs were seeded into six-well plates at a density of $5x10^4$/ml, followed by the addition of Pam3CSK4 (1 μmol/l) or C29 (1 μmol/l) for 24 h. The cells were collected and stained using an Annexin V-FITC/PI kit (cat. no. C1062L; Beyotime Institute of Biotechnology) according to the manufacturer's protocol. The HUVECs were exposed to 5 μl of Annexin V-FITC and 10 μl of PI solution for 15 min in the dark. After staining, the cells were run on a Gallios flow cytometer (Beckman Coulter, Inc.) and the data were analyzed using the Kaluza software (perpetual A82959; Beckman Coulter, Inc.).

Reverse transcription-quantitative (RT-q) PCR. Total RNA from fresh deep vein tissues from model animals and HUVECs ($1x10^6$/well in 6-well plates) was extracted using TRIzol® reagent (Thermo Fisher Scientific, Inc.) according to the manufacturer's protocol. Additionally, 1 μg RNA was reverse transcribed into cDNA using the HI Script Q RT SuperMix (Vazyme Biotech Co., Ltd.) according to the manufacturer's instructions. RT-qPCR was performed using the cDNA templates and SYBR (Takara Bio, Inc.) in a Bio-Rad CFX96 system (Bio-Rad Laboratories, Inc.). Specific primers for TLR2, TF and IL-6 were designed and synthesized according to the GenBank (National Center for Biotechnology Information) sequences. RT-PCR was performed using Maxima SYBR Green qPCR Master Mix (cat. no. K0251; Thermo Fisher Scientific, Inc.). RT-PCR was performed using Maxima SYBR Green qPCR Master Mix (cat. no. K0251; Thermo Fisher Scientific, Inc.). The PCR cycling conditions were: denaturation at 95˚C for 30 sec, annealing at 60˚C for 30 sec and extension at 72˚C for 30 sec, for a total of 40 cycles. Gene expression levels were calculated using the $2^{-\Delta\Delta Cq}$ method (24), normalized to GAPDH. The experiments were replicated three times. The primer sequences are listed in Table I.

Western blot analysis. Total protein was extracted from HUVECs and vessel tissues using radioimmunoprecipitation assay buffer (Beijing Solarbio Science & Technology Co., Ltd.) supplemented with protease and phosphatase inhibitors (Thermo Fisher Scientific, Inc.). The protein concentration was determined using the BCA Protein Assay Kit (cat. no. 71285-M; MilliporeSigma) following the manufacturer's protocol. For western blot analysis, 50 μg of lysate was loaded onto sodium dodecyl sulfate-polyacrylamide gel electrophoresis gels, transferred onto polyvinylidene difluoride membranes (MilliporeSigma). Equal amounts of proteins were resolved on 10% SDS-PAGE gels and blotted to polyvinylidene difluoride membranes. The membranes were blocked in 5% not-fat dry milk at room temperature for 1 h and incubated overnight with

primary antibodies (1:1,000) against TLR2 (cat. no. ab213676; Abcam, Cambridge, UK), NF-kB p65 (cat. no. ab16502; Abcam) and IL-6 (cat. no. ab233706; Abcam). After retrieval of the primary antibody, the membranes were washed thrice with 1XTris-buffered saline with 0.1% Tween 20 for 5 min each. Secondary antibodies conjugated with horseradish peroxidase were diluted 1:1,000 according to the corresponding specifications. Incubation with secondary antibodies was conducted at 4˚C overnight or at room temperature for 4 h. Secondary antibodies (1:3,000; cat. nos. 31460 and 31430; Thermo Fisher Scientific, Inc.) were incubated at room temperature for 1 h. Proteins were visualized using an ECL reagent (cat. no. 34580; Thermo Fisher Scientific, Inc.) Densitometry analysis was performed using Quantity One Software and quantified relative to the loading control, β-actin. Image analysis was performed using Image-Pro Plus software (version 6.0; Media Cybernetics, Inc.).

Immunofluorescence staining. NF-κB translocation in the vein tissues and HUVECs was determined using an NF-κB Activation, Nuclear Translocation Assay Kit (cat. no. SN368; Beyotime Institute of Biotechnology) according to the manufacturer's instructions. HUVECs were seeded onto slides at a density of $1x10^4$ cells per slide. After fixation with 4% paraformaldehyde for 15 min at room temperature (approximately 25˚C). Cells were permeabilized with 0.1% Triton X-100 in PBS for 10 min at room temperature. he sections and cells were blocked with 3% bovine serum albumin (BSA; cat. no. A7030; MilliporeSigma) for 1 h. The samples were incubated with primary antibodies, including an NF-κB antibody (1:200, cat. no. ab16502; Abcam) and TLR2 antibody (1:200, cat. no. ab213676; Abcam) for 1 h at room temperature. They were then washed thrice with phosphate-buffered saline (PBS) for 5 min each time. The samples were incubated with a secondary antibody solution (1:500, goat anti-rabbit IgG, cat. no. A-11008; Invitrogen) for 1 h at room temperature. The sections and cells were treated with DAPI solution (1 μg/ml, cat. no. D9542; MilliporeSigma) for 5 min at room temperature. An antifluorescence quencher (cat. no. P0126; Beyotime Institute of Biotechnology) was added. Images were captured under a laser confocal fluorescence microscope (FV1200; Olympus Corporation) at a magnification of 40x and analyzed using Image-Pro Plus software (version 6.0; Media Cybernetics, Inc.).

Hematoxylin and eosin (H&E). For histological examination, tissues were fixed with 4% paraformaldehyde at room temperature for 24 h, washed with 70% alcohol, dehydrated through a graded ethanol series (70, 80, 95, and 100%, 10 min each), and cleared in xylene (two changes, 10 min each). Tissues were embedded in paraffin and cut into 4 μm sections. Sections were deparaffinized in xylene (two changes, 10 min each), rehydrated through a graded ethanol series (100, 95, 80, and 70%, 5 min each), and rinsed in distilled water. Hematoxylin staining was performed at room temperature for 5 min, rinsed in running tap water for 5 min, followed by eosin staining at room temperature for 2 min. Sections were then dehydrated through a graded ethanol series and cleared in xylene. Images were acquired under a light microscope (DM 2500; Leica Microsystems GmbH).

Table II. Thrombosis rate in each group.

Group	Cases of thrombosis	Cases without thrombosis	Total	Thrombosis rate (%)
Sham	0	7	7	0
Model	3	4	7	42.8
Pam3csk4	6	1	7	85.7
C29	2	5	7	28.6
Total	12	16	28	

Statistical analysis. Results were presented as mean ± SD and calculated using the SPSS 21.0 software (IBM Corp.) and GraphPad Prism 8.0 (Dotmatics). One-way ANOVA test was employed followed by Tukey post hoc test. $P<0.05$ was considered to indicate a statistically significant difference.

Results

TLR2 activation promotes DVT whereas TLR2 inhibition of reduces DVT in a TDVT model. A DVT model was first established using the quantitative impact and gypsum fixation method (plaster cast) and X-ray examination was performed to examine the effect (Fig. 1A). After successful modeling, the number of thrombus formation cases in each group as well as the length and weight of deep vein thrombosis were compared (Table II). Inflammation was evaluated via hematoxylin and eosin staining of the tissue samples (Fig. 1B). The number of thrombus formation cases, as well as the weight and length of the thrombi, were higher in the Pam3CSK4 group compared with the model and C29 groups (Fig. 1C-E). This indicated that TLR2 activation increases the incidence of DVT in TDVT model rats, whereas TLR2 inhibition reduces DVT incidence.

TLR2 expression is increased in the TDVT model group and is positively correlated with NF-κB phosphorylation. TLR2 expression was higher in the model group and NF-κB phosphorylation was positively correlated with TLR2 expression. To verify the relationship between TLR2 and its downstream molecules in the TDVT model, immunofluorescence staining, PCR and western blotting of TDVT tissues were conducted. Immunofluorescence staining of TLR2 in the vascular tissues of the animal model showed that TLR2 expression was significantly higher in the model group than in the sham group. In addition, TLR2 expression was significantly higher in the model + Pam3CSK4 group than in the model + C29 group (Fig. 2A and C). The present study also found a positive correlation between NF-κB expression and TLR2 expression as well as intergroup differences in expression (Fig. 2B and D). qPCR revealed that compared with those in the model group, the vascular EC of rats in the model + Pam3CSK4 and model + C29 groups had an increased transcription of TLR2 and the differences were significant ($P<0.05$; Fig. 2E). These results were confirmed by western blotting, which showed that TLR2 expression was positively correlated with P-65 and phosphorylated (p-)P65 expression in the TDVT animal model (Fig. 2F-I).

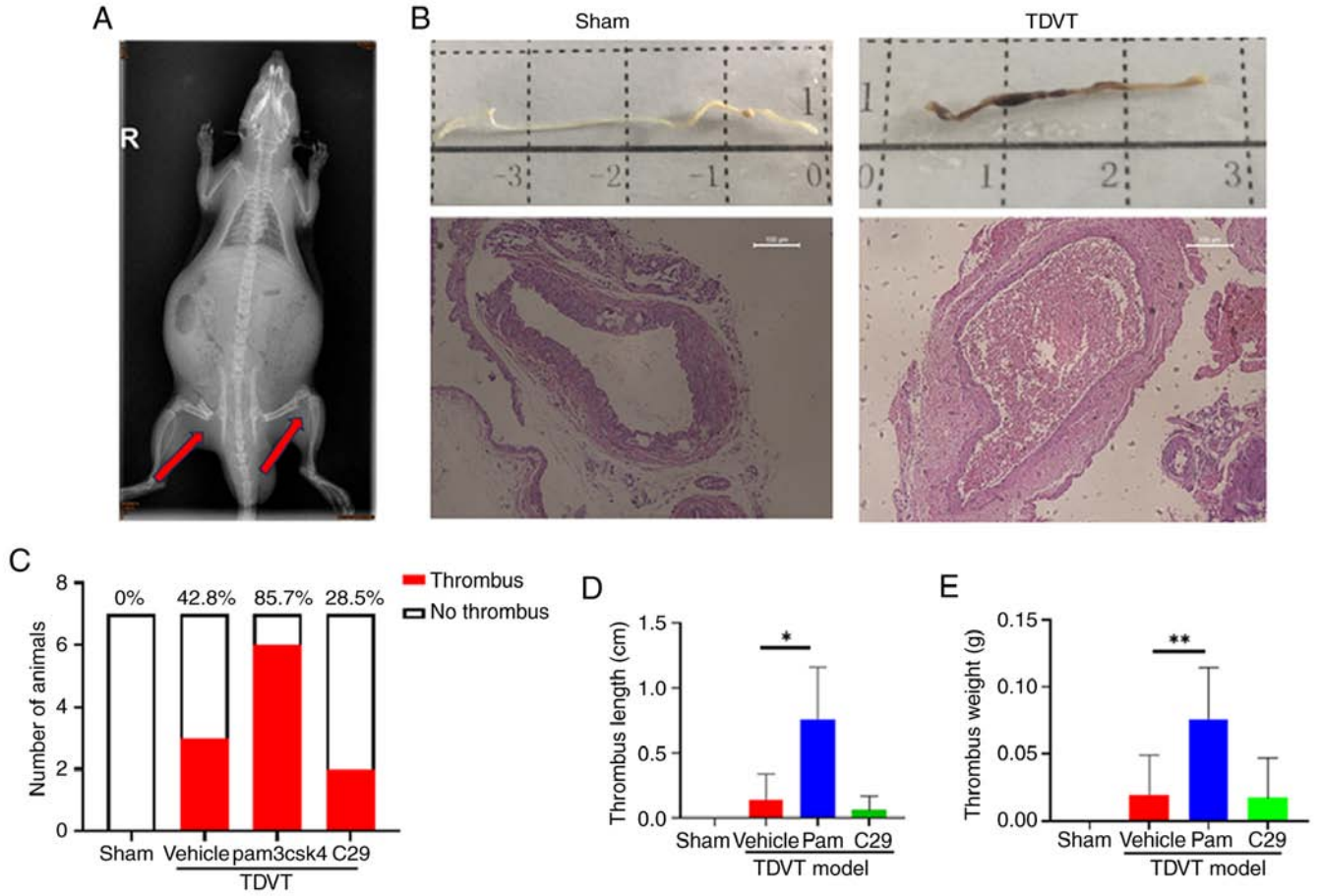

Figure 1. Establishment of an animal model to simulate TDVT formation using quantitative impact method. (A) Representative image of the TDVT model established in rats (X-ray image). (B) Histological sections of rat femoral veins after modeling and hematoxylin and eosin staining. The images at the top shows the gross specimen, displaying the extracted deep vein without thrombosis, the deep vein with thrombosis, and the thrombus within it, all after fixation with paraformaldehyde. (C) The rates of DVT formation in different groups, where the sham group did not form thrombi, the model group had a thrombus formation rate of 42.8%, the pam3csk4 group had a thrombus formation rate of 85.7% and the C29 group had a thrombus formation rate of 28.5%. (D) The length of thrombus formed in different groups as observed in gross specimens, where there was a statistically significant difference in thrombus length between the sham group and the pam3csk4 group ($P<0.05$), between the model group and the pam3csk4 group ($P<0.05$) and between the sham group and the pam3csk4 group ($P<0.05$). (E) The weight of thrombus formed in different groups as observed in gross specimens, where there was a statistically significant difference in thrombus weight between the sham group and the pam3csk4 group ($P<0.05$), between the model group and the pam3csk4 group ($P<0.05$) and between the sham group and the pam3csk4 group ($P<0.05$). All data were expressed as the mean ± SD. One-way ANOVA followed by Tukey's test, $^{*}P<0.05$, $^{**}P<0.01$, n=7. TDVT, traumatic deep vein thrombosis.

The downstream molecules of TLR2/NF-κB in the TDVT model are IL-6, COX-2 and P-selectin. To validate the relationship between TLR2 and its downstream molecules in the TDVT model, the PCR and western blotting data from the tissues of the TDVT animal model were analyzed. It was found that TLR2 expression was significantly higher in the model group than in the sham group, along with a significant increase in the gene expression of IL-6, COX-2 and P-selectin. In the model + Pam3CSK4 group, the gene expression levels of IL-6, COX-2, P-selectin and TF were significantly higher than those in the model + C29 group (Fig. 3A and D). Western blotting analysis revealed that the protein levels of IL-6 and COX-2 in the TDVT model were higher than those in the sham group. Furthermore, TLR2 activation led to an increase in protein levels, whereas TLR2 inhibition resulted in a significant decrease in protein levels (Fig. 3E-G). Based on these results, it was considered that IL-6, COX-2 and P-selectin are the downstream molecules of TLR2/NF-κB in the TDVT model.

Validation of changes in the TDVT model caused by EC. To validate the specific cellular changes responsible for alterations in thrombus formation in the TDVT model, the present study focused on EC injury induced by inflammation as a key factor in TDVT pathogenesis. EC are an important component of the vascular wall that maintain the integrity and normal blood flow of the vessel by controlling platelet activity and clotting factors in the blood. The present study used HUVECs and established an OGD model for analysis. The appropriate drug concentration for experimentation was determined using the CCK8 method. Pam3CSK4 at 1 μmol/l showed inhibitory effects on HUVECs and this effect increased with increasing Pam3CSK4 concentration. At low concentrations, C29 promoted HUVEC proliferation, but it peaked at 1 μmol/l and then declined. Pam3CSK4 and C29 both had the most significant promoting or inhibitory effects at 1 μmol/l and the differences compared with the control group were significant (Fig. 4A). In addition, the effects of TLR2 activation and inhibition on EC apoptosis under OGD conditions were observed.

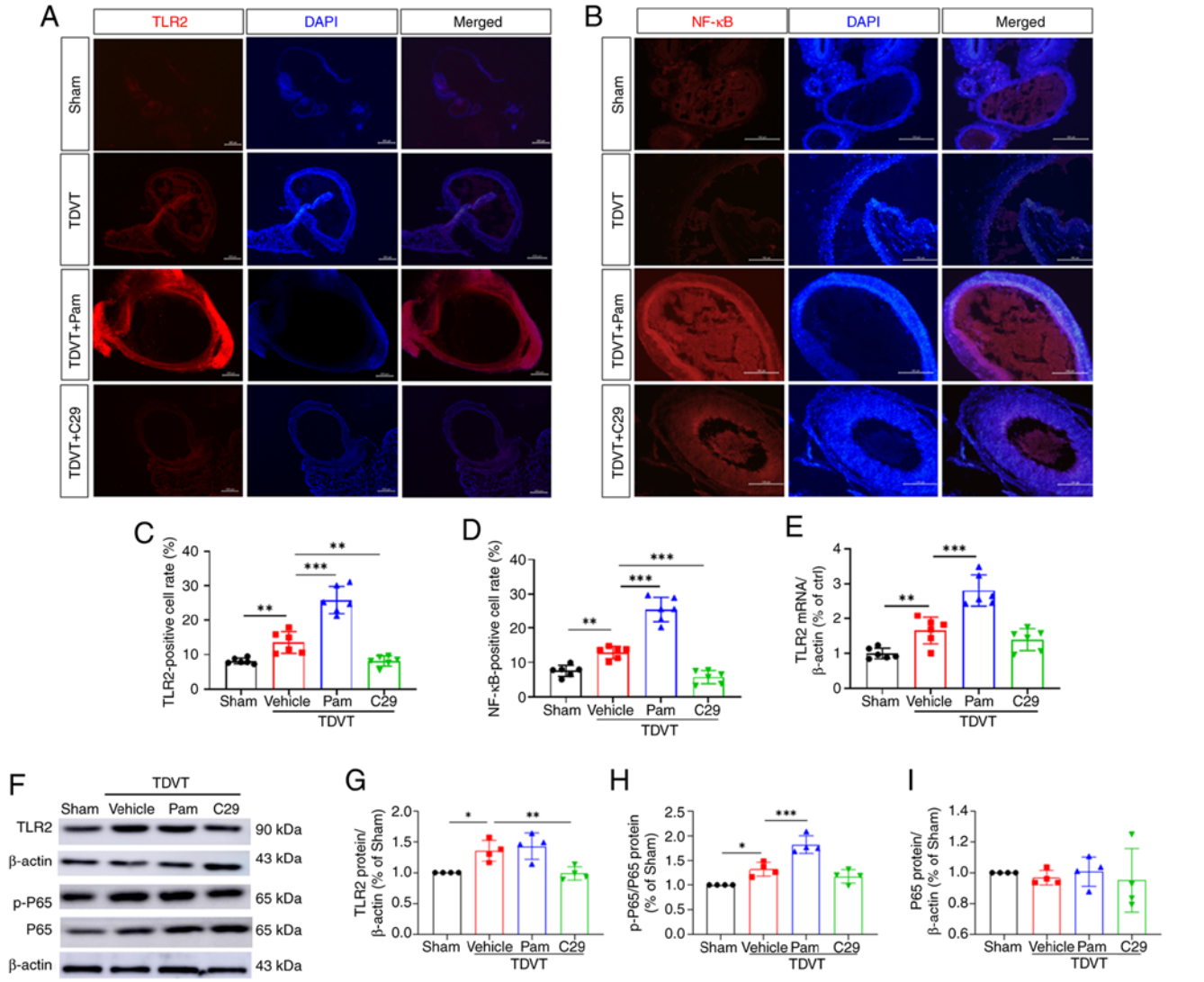

Figure 2. TLR2/NF-κB signaling were activated in the deep veins of the TDVT model animals. (A and B) Immunofluorescence results of TLR2 and NF-κB in the deep vein tissues, magnification, x20. (C and D) TLR2 and NF-κB positive cell rate. (E) Relative mRNA expression of TLR2 in the deep vein tissues. (F-I) Relative protein levels of TLR2, p-P65 and P65 in the deep vein tissues. All data were expressed as the mean ± SD. One-way ANOVA followed by Tukey post hoc test, *P<0.05, **P<0.01 and ***P<0.001. TLR2, Toll-like receptor; NF-κB, nuclear factor kappa B; TDVT, traumatic deep vein thrombosis; p-, phosphorylated; Pam, Pam3CSK4.

It was found that the apoptosis rate in the vehicle group was significantly higher than that in the control group but was lower than that in the Pam3CSK4 (Fig. 4B-D).

The downstream molecules of TLR2/NF-κB in the OGD model are IL-6, COX-2 and P-selectin. To verify the relationship between TLR2 and its downstream molecules in the HUVEC OGD model, PCR analysis weas performed. It was found that IL-6 expression increased in the vehicle group compared with the sham group and that the gene expression of IL-6, COX-2, P-selectin and TF increased significantly. In the model + Pam3CSK4 group, the gene expression of IL-6, COX-2, P-selectin and TF was significantly higher than that in the model + C29 group (Fig. 5A-D). Western blotting revealed that the protein levels of IL-6 and COX-2 in the TDVT model were higher than those in the sham group. TLR2 activation increased their protein levels, whereas TLR2 inhibition significantly decreased their levels (Fig. 5E-G). These results indicate that IL-6, COX-2 and P-selectin are the downstream molecules of TLR2/NF-κB.

Immunofluorescence reveals that IL-6, COX-2 and P-selectin are the downstream molecules of TLR2/NF-κB in the OGD model. To investigate the relationship between TLR2 and its downstream molecules in the HUVEC OGD model, immunofluorescence staining, PCR and western blotting analysis were performed. Immunofluorescence staining of TLR2 in the vein tissue of the cellular OGD model showed that TLR2 expression significantly increased in the vehicle group compared with that in the sham group. TLR2 expression in the OGD + Pam3CSK4 group was significantly higher than that in the OGD + C29 group (Fig. 5A and C). Meanwhile, NF-κB expression was positively associated with TLR2 expression and showed intergroup differences (Fig. 5B and D). qPCR showed that the transcription level of TLR2 in the EC of the model + Pam3CSK4 group was greater than that in the model group. The transcription levels of TLR2, P65 and p-P65 genes in the EC of the model + C29 group were higher than that in the model group. The differences between the two groups were significant (P<0.05;

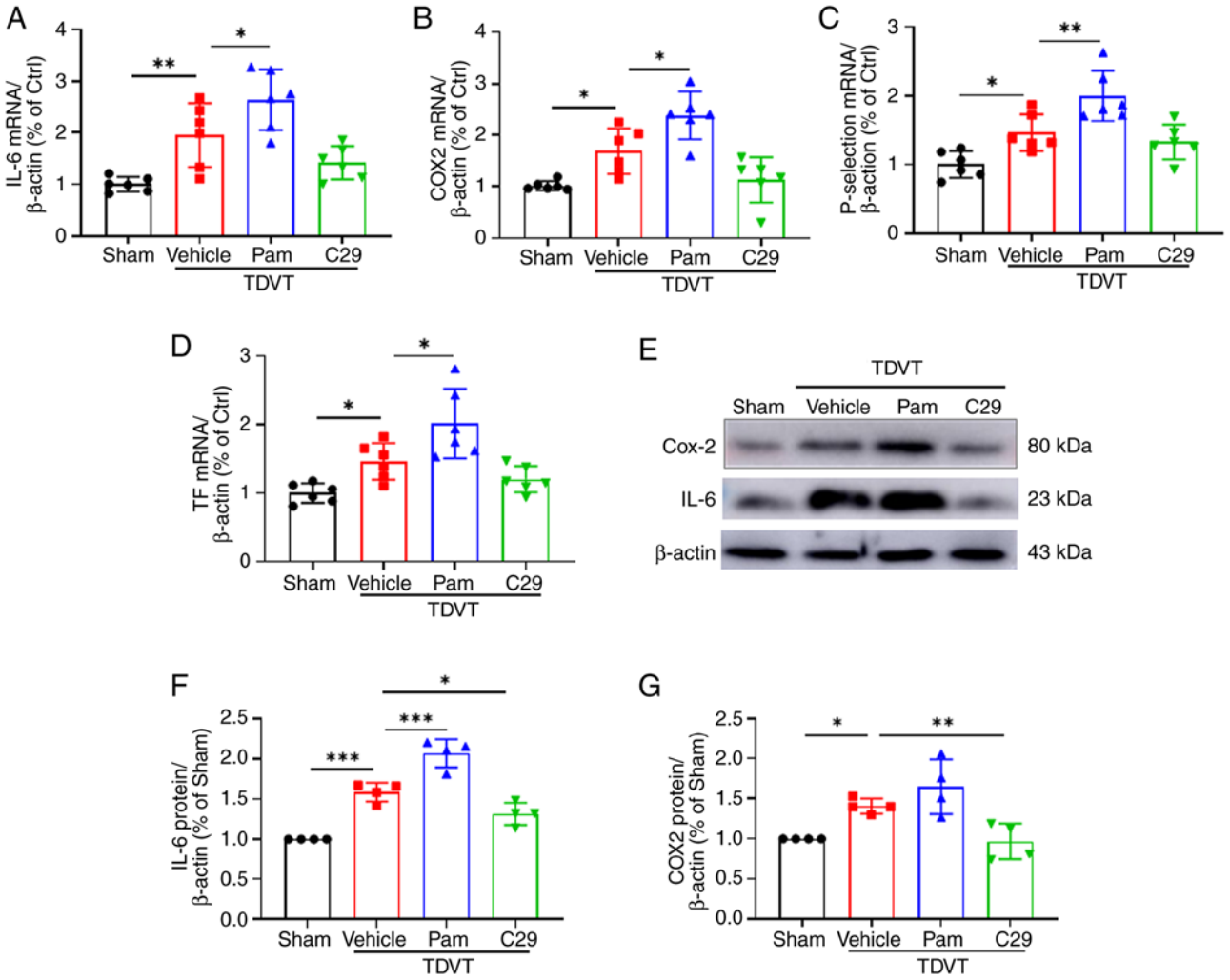

Figure 3. The Comparison of DVT lengths, weight and the rate of thrombosis among different groups. (A-D) Comparison of IL-6, COX2, P-selectin and TF mRNA expression among different groups. (E-G) Comparison of Expression of COX2 and IL-6 protein levels among different groups. All data were expressed as the mean ± SD. One-way ANOVA followed by Tukey test, *P<0.05, **P<0.01 and ***P<0.001, n=4-6. DVT, deep vein thrombosis; COX-2, cyclooxygenase-2; TF, tissue factor.

Fig. 6E). Similar results were obtained in western blotting, which showed a positive correlation between TLR2 expression and the gene expression of P65 and p-P65 in the TDVT animal model (Fig. 6F-I).

Discussion

TVDT is a prevalent complication of severe trauma or surgery and is a serious threat to human health. Currently, the diagnosis and treatment of DVT remain at the stage of coagulation function examination and post-onset treatment. The consequences of the onset of TVDT impose a heavy burden on patients. Therefore, identifying the pathogenesis of TDVT is an important research direction for improving its diagnosis and treatment. Studies have shown that DVT and inflammation have similar cellular signaling pathways and that inflammation significantly contributes to the development of TVDT (2,23). TLR2/NF-κB is a common inflammatory signaling pathway. TLR2 is a potential target for inflammatory injury in various EC and this mechanism may be related to the enhanced TLR2 activation of NF-κB (3).

Vascular EC are multifunctional cells on the inner side of the vascular wall that have important regulatory functions in various physiological and pathological processes, such as thrombosis, inflammation, immunity, angiogenesis and substance transport (3). Their basic function is to maintain unobstructed blood flow in blood vessels (24). Recent studies have found that in a mouse model of DVT, a process of acute to chronic inflammation in the vein walls occurs (5). These results suggested that inflammation is closely associated with DVT. When inflammation causes the activation of inflammatory cytokines, the release of a large number of inflammatory mediators damages EC in the vascular wall (3). Simultaneously, large amounts of TF, von Willebrand factor, adhesion molecules and cytokines are released (6) and the anti-adhesion, anticoagulant, vasodilator and anti-inflammatory phenotypes are transformed into activated states, thus promoting adhesion, coagulation and inflammation. In addition, EC injury can cause leukocyte aggregation and platelet adhesion, aggregation and activation, which causes blood to be in a hypercoagulable state, leading to an imbalance in the coagulation and fibrinolysis systems, thus promoting the

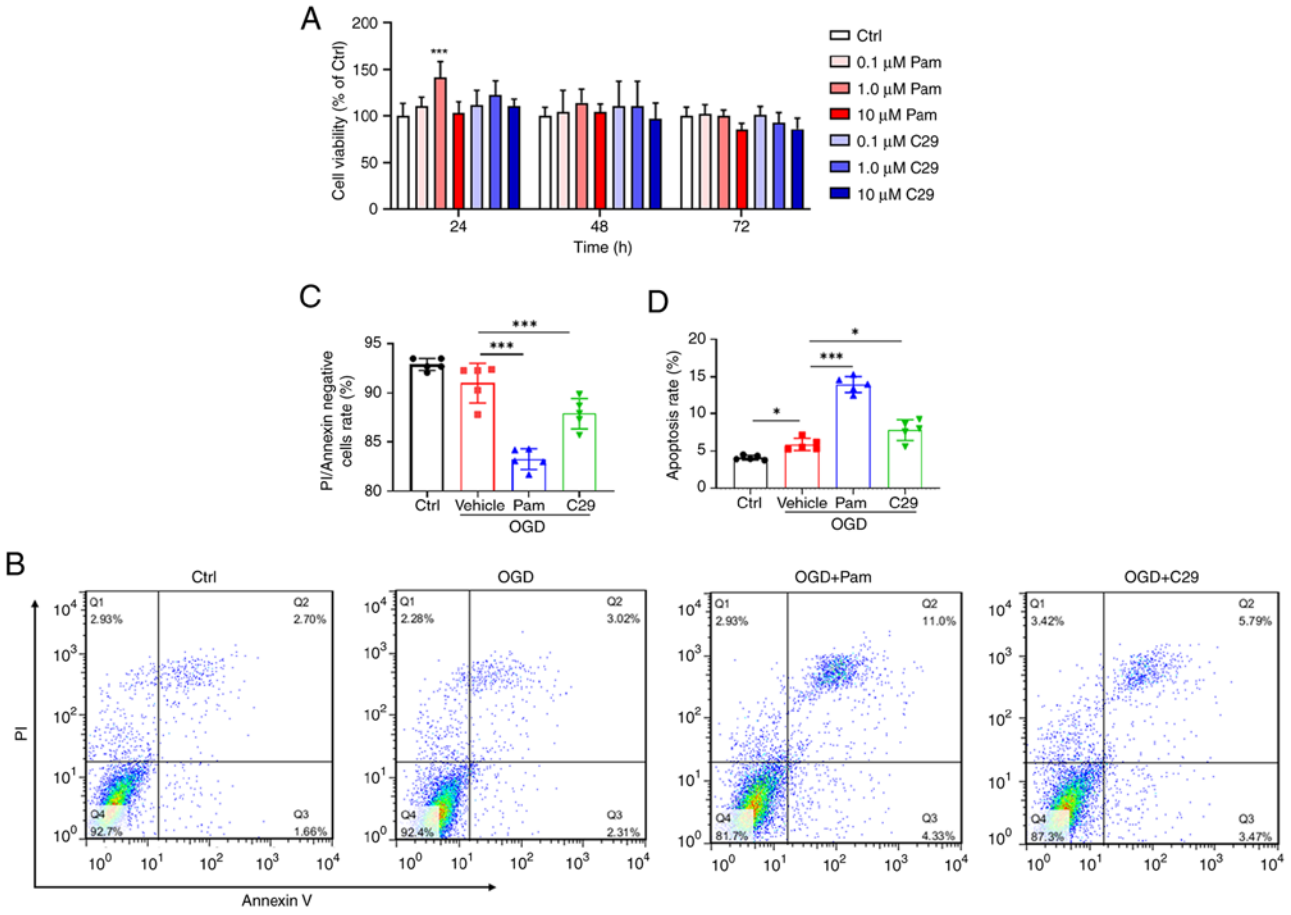

Figure 4. Comparison of cell viability and apoptosis among different groups. (A) CCK-8 assay was used to determine the tolerance of HUVECs to different concentrations of Pam and C29. (B) Flow cytometry plots of different groups. (C) Normal cell ratios of HUVECs in different groups. (D) Normal cell ratios of HUVECs in different groups. All data were expressed as the mean ± SD. One-way ANOVA followed by Tukey test, *P<0.05 and ***P<0.001, n=5. Ctrl, control; HUVECs, human umbilical vein endothelial cells; Pam, Pam3CSK4.

occurrence and development of DVT (8,11). Therefore, the structural and functional integrity of the vascular EC largely determines thrombosis.

Evidence has shown that TLR2 may be a potential target for inflammatory injury in various EC (11). Other studies have suggested that the expression of COX-2 is regulated by the NF-κB signaling pathway (9). Studies on TLR2 signaling molecules have mostly focused on atherosclerosis (9,10), osteoarthritis (25) and tumors (26). Some studies have analyzed changes in the expression of TLR2, NF-κB and COX-2 in DVT samples using bioinformatics analysis (10,11,26) and preliminarily found that the three molecules are closely related to thrombosis.

TLRs are transmembrane proteins that belong to the pattern recognition receptor family and are highly evolutionarily conserved (27). Studies have shown that TLR2 and TLR4 are the most important molecules involved in TLR-mediated inflammatory responses, with TLR2 being mainly distributed in immune cells such as monocytes, macrophages and EC (11,13). When the blood flow status in the blood vessel changes (such as in a case of turbulence), the TLR2 distributed in EC is easily activated and its expression increases rapidly (14). The inflammatory response induced by TLRs (except TLR3) is widely considered to occur through a classical signaling pathway that starts from a conserved intracellular sequence of TLRs, the Toll/IL-1 receptor homologous region (14,28), which can activate mitogen-activated protein kinase (MAPK) and IκB kinase, further activating the expression of inflammatory factors induced by NF-κB (11,29).

NF-κB is a downstream molecule of TLR2, wherein transcription-dependent NF-κB binds to MYD88 and MAL to activate related kinases, further phosphorylating IKB and releases the P50 and p65 subunits of the NF-κB molecule, thereby causing an inflammatory reaction and facilitating gene transcription (11,27). In an independent pathway of NF-κB transcription, nuclear translocation of activated NF-κB can directly cause inflammatory reactions and guide the transcription of related genes. In addition, NF-κB can be activated by a variety of stimulants, such as cytokines, growth factors, bacterial or viral products and reactive oxygen species (30). The activated NF-κB, its double-stranded DNA and the MAPK system further activate EC, promoting the expression of inflammatory mediators such as ICAM-1, VCAM-I and E-selectin and increasing the expression of inflammatory mediators such as TNF-α, IL-1, IL-6, IL-8 and IL-17, which amplify the inflammatory effect (31-33). TNF-α, IL-1 and CD40 can induce the expression of TF in EC and monocytes (29,34) and NF-κB can mediate the activation of TF in vascular smooth muscle cells and venous vascular EC, thus playing an important role in venous thrombosis (32).

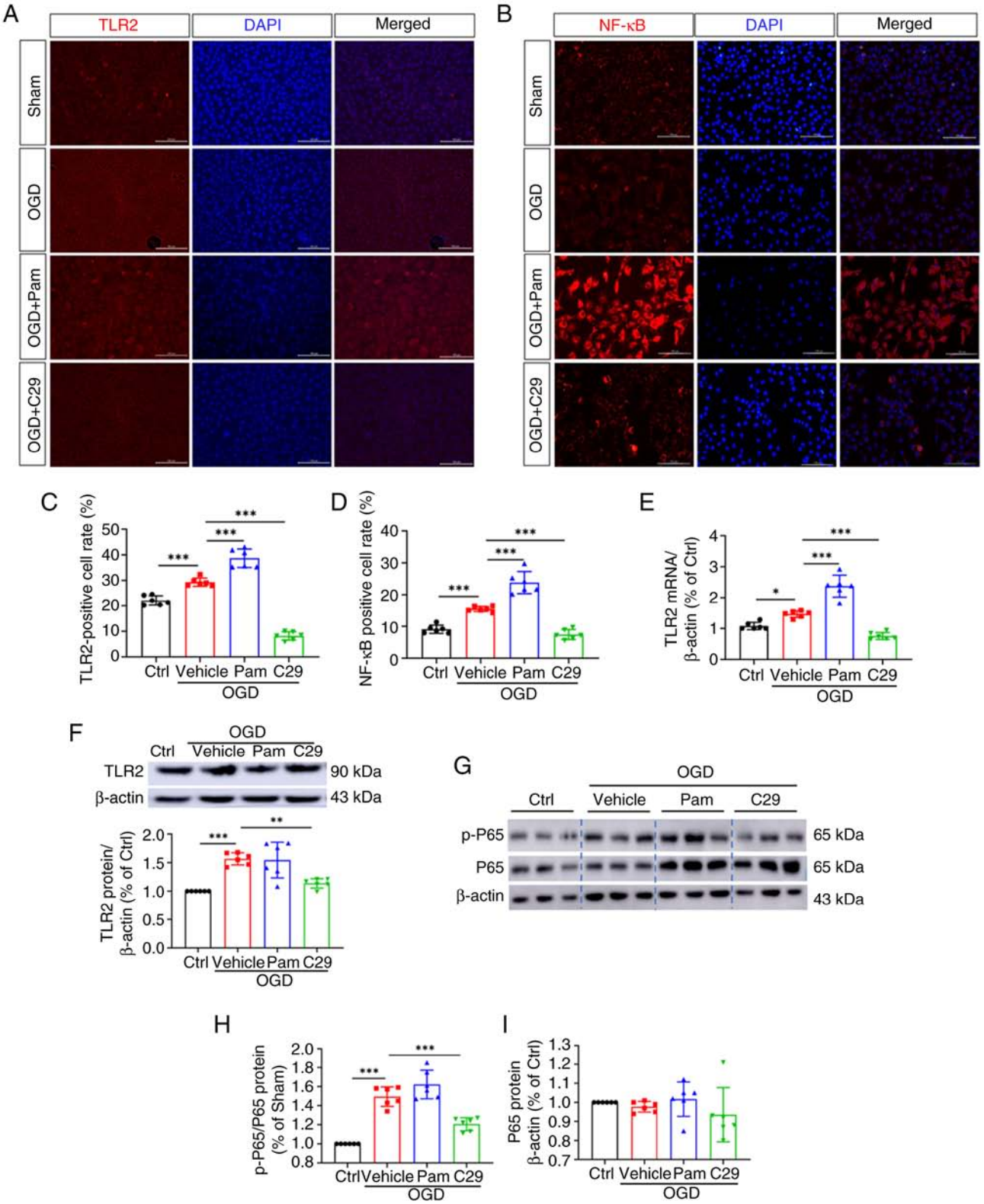

Figure 5. TLR2/NF-κB signaling were activated in HUVECs after OGD injury. Immunofluorescence results of (A) TLR2 and (B) NF-κB in HUVECs (magnification, x100), (C and D) TLR2 and NF-κB positive cell rate. (E) Relative mRNA levels of TLR2 in HUVECs. (F-I) Relative protein levels of TLR2, p-P65, P65 in HUVECs. All data were expressed as the mean ± SD. One-way ANOVA followed by Tukey test, *P<0.05, **P<0.01 and ***P<0.001, n=6. TLR2, Toll-like receptor 2; NF-κB, nuclear factor kappa B; OGD, oxygen glucose deprivation; HUVECs, human umbilical vein endothelial cells; Ctrl, control; Pam, Pam3CSK4.

COX-2 is an inducible enzyme that is generally not expressed in normal tissues but is highly expressed when cells are stimulated by cancer-promoting agents, inflammatory mediators, cytokines and growth factors (9). COX-2 has NF-κB binding sites that mediate COX-2 expression (9). The latter promotes the oxidative stress response, leading to the

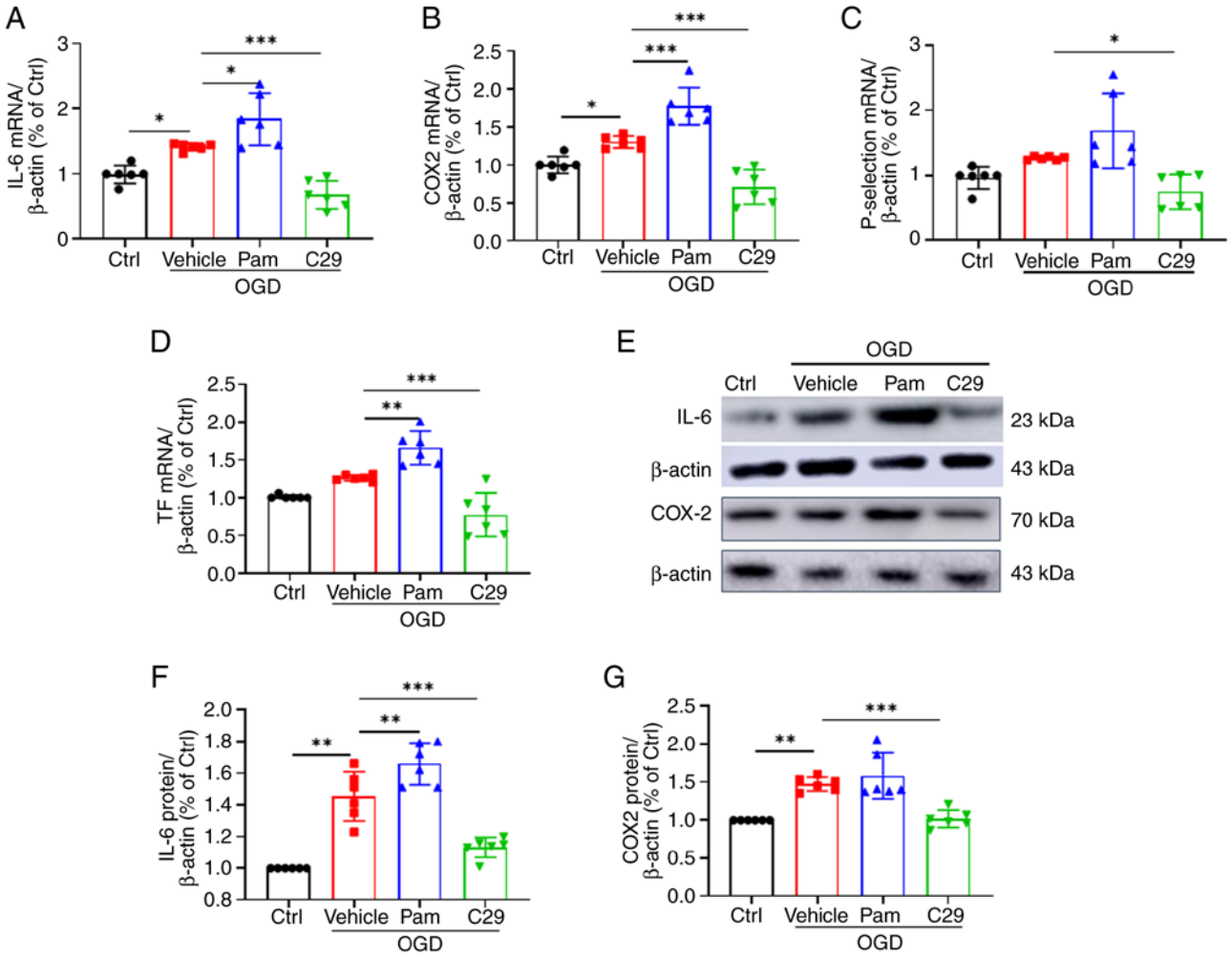

Figure 6. Downstream molecules of TLR2/NF-κB in the OGD model. Relative mRNA expressions of (A) IL-6, (B) COX-2, (C) P-selectin and (D) TF in different groups of HUVECs. (E-G) Relative protein levels of IL-6 and COX-2 in different groups of HUVECs. All data were expressed as the mean ± SD. One-way ANOVA followed by Tukey test, *P<0.05, **P<0.01 and ***P<0.00, n=6. Toll-like receptor 2; NF-κB, nuclear factor kappa B; OGD, oxygen glucose deprivation; COX-2, cyclooxygenase-2; HUVECs, human umbilical vein endothelial cells; Ctrl, control; Pam, Pam3CSK4; Tissue Factor.

accumulation of reactive oxygen species and can convert arachidonic acid into prostaglandins (PGE2), which are important factors in inflammatory diseases (10). PGE2 is a key proinflammatory factor that induces the release of chemokines from inflammatory cells, recruits inflammatory cells and cooperates with lipopolysaccharides to induce the expression of IL-6 and IL-1 in macrophages. PGE2 expression promotes platelet activation and thrombosis (10).

As aforementioned, TLR2/NF-κB is a common inflammatory signaling pathway. TLR2 has been shown to be a potential target for inflammatory injury in various EC (32). The mechanism may be related to enhanced TLR2 activation of NF-κB.

In the present study, the thrombus formation rate in the Pam3CSK4 group (85.71%) was significantly higher than those in the model (57.14%) and TLR2 inhibition (28.57%) groups. These results indicated that the TLR2 agonist Pam3CSK4 promoted TDVT development, whereas the TLR2 inhibitor C29 inhibited TDVT development. This suggests that TLR2 may be involved in an important mechanism in TVDT and may promote venous thrombus formation. Literature review and preliminary bioinformatics analysis revealed that the key downstream molecules of TLR2 may include NF-κB, COX-2, IL-6 and TF (9-11). By establishing a rat model of TDVT to simulate *in vivo* conditions, the OGD experiment mimicked the ischemic-hypoxic environment of vascular EC during thrombus formation. It was observed that with an increase in TLR2 expression in the *in vivo* and *in vitro* experiments, NF-κB p-NF-κB (p-P65) expression increased. In the HUVEC OGD model, TLR2 expression increased under ischemic-hypoxic conditions and NF-κB translocated from the cytoplasm to the nucleus. Key molecules in the TLR2 signaling pathway, TLR2/NF-κB/COX-2/IL-6, changed with TLR2 regulation. Therefore, it was hypothesized that TLR2/NF-κB/COX-2/IL-6 is one of the signaling pathways involved in TVDT. In the *in vivo* experiments, it was also observed that, compared with the control group, the levels of TLR2, IL-6, COX-2 and p-P65 were significantly higher in the model group. The thrombus formation rate in the Pam3CSK4 group was higher and the levels of TLR2, IL-6 and COX-2 increased. In addition, the levels of the aforementioned indicators in the C29 group were significantly relatively lower compared with those in the control group. Thus, it can be inferred that TLR2, IL-6 and COX-2 are upregulated during DVT.

The present study observed a positive correlation between the expression of IL-6 and COX-2 and the activation and inhibition of TLR2. In *in vivo* experiments, IL-6 and COX-2 levels significantly increased when TLR2 was activated and were positively correlated with thrombosis. It was hypothesized that IL-6, COX-2 and other molecules play important roles as signal transducers and chemokines in DVT.

To gain a comprehensive understanding of the mechanisms underlying TDVT formation, future research endeavors should encompass a broader examination of changes within the systemic environment. By investigating the interplay of these factors, the intricate pathways involved in thrombus formation can be more clearly elucidated. Such investigations will pave the way for the development of more effective prevention and treatment strategies for this clinically significant condition.

In conclusion, increased TLR2 expression was found in the TDVT model. TLR2 was positively correlated with the molecular contents of IL-6, NF-κB and COX-2. TLR2/NF-κB/COX-2 is one of the possible signaling pathways in TDVT. Further research on the signaling pathways in TDVT is of great significance for an in-depth understanding of the condition as well as the selection of therapeutic targets and development of new drugs. It may also provide new clues for clinical prophylactic medication and treatment of TDVT, which has important theoretical and practical significance.

Acknowledgements

The authors thank Dr Limei Zhang, Dr Xuanfeng Wang (Department of Pathology of Gannan Medical University, Ganzhou, China) and Professor Minhong Zhang (Affiliated Hospital of Gannan Medical University, Ganzhou, China) for technical support and for supporting histological processing, sectioning and staining and Xiaozhu Wu (Affiliated Hospital of Gannan Medical University, Ganzhou, China) for taking X-rays.

Funding

The present study was supported by grants from the National Natural Science Foundation of China (grant no. 82160375), the Natural Science Foundation of Jiangxi Province (grant no. 20202BABL206035), the Science and Technology Program of Jiangxi Provincial Administration of Traditional Chinese Medicine (grant no. 2021A374), the Science and Technology Planning Project of Jiangxi Provincial Health Commission in 2023 (grant no. 202312146) and the Ganzhou Municipal Science and Technology Plan Project (grant no. 2023LNS26841).

Availability of data and materials

The data generated in the present study may be requested from the corresponding author.

Authors' contributions

TG conceived and designed the experiments, performed the experiments, analyzed the data, prepared figures and tables, LX wrote and reviewed drafts of the article and approved the final draft. JX and JZ prepared figures and performed analysis and interpretation of data. MY and ZH prepared figures and contributed to manuscript revisions. TG and JM confirm the authenticity of all the raw data. JM and XZ, as corresponding authors, edited and approved the final draft. All authors read and approved the final manuscript.

Ethics approval and consent to participate

All animal procedures were performed following the guidelines of the Council on Animal Care and were approved by the Gannan Medical Ethics Committee (Ganzhou, China; approval no. LLSC-2022110701).

Patient consent for publication

Not applicable.

Competing interests

The authors declare that they have no competing interests.

References

1. Scolaro JA, Taylor RM and Wigner NA: Venous thromboembolism in orthopaedic trauma. J Am Acad Orthop Surg 23: 1-6, 2015.
2. Wu L and Cheng B: Analysis of perioperative risk factors for deep vein thrombosis in patients with femoral and pelvic fractures. J Orthop Surg Res 15: 597, 2020.
3. Fan J, Zhou F, Xu X, Zhang Z, Tian Y, Ji H, Guo Y, Lv Y, Yang Z and Hou G: Clinical predictors for deep vein thrombosis on admission in patients with intertrochanteric fractures: A retrospective study. BMC Musculoskelet Disord 22: 328, 2021.
4. He LX, Xie JY, Lv J, Liu H, Liao DB, Wang GL, Ning N and Zhou ZK: Quality evaluation of clinical practice guidelines for thromboprophylaxis in orthopaedic trauma based on AGREE II and AGREE-REX: A systematic review protocol. BMJ Open 12: e59181, 2022.
5. Whiting PS, White-Dzuro GA, Greenberg SE, VanHouten JP, Avilucea FR, Obremskey WT and Sethi MK: Risk factors for deep venous thrombosis following orthopaedic trauma surgery: An analysis of 56,000 patients. Arch Trauma Res 5: e32915, 2016.
6. Di Minno A, Frigerio B, Spadarella G, Ravani A, Sansaro D, Amato M, Kitzmiller JP, Pepi M, Tremoli E and Baldassarre D: Old and new oral anticoagulants: Food, herbal medicines and drug interactions. Blood Rev 31: 193-203, 2017.
7. Alhassan S, Pelinescu A, Gandhi V, Naddour M, Singh AC and Bihler E: Clinical presentation and risk factors of venous thromboembolic disease. Crit Care Nurs Q 40: 201-209, 2017.
8. Colling ME, Tourdot BE and Kanthi Y: Inflammation, infection and venous thromboembolism. Circ Res 128: 2017-2036, 2021.
9. Du X, He S, Jiang Y, Wei L and Hu W: Adiponectin prevents islet ischemia-reperfusion injury through the COX2-TNFα-NF-κB-dependent signal transduction pathway in mice. J Endocrinol 218: 75-84, 2013.
10. Lee SY, Kim MH, Kim SH, Ahn T, Kim SW, Kwak YS, Cho IH, Nah SY, Cho SS, Park KM, *et al*: Korean Red Ginseng affects ovalbumin-induced asthma by modulating IL-12, IL-4, and IL-6 levels and the NF-κB/COX-2 and PGE(2) pathways. J Ginseng Res 45: 482-489, 2021.
11. Pinheiro CR, Coelho AL, de Oliveira CE, Gasparoto TH, Garlet GP, Silva JS, Santos CF, Cavassani KA, Hogaboam CM and Campanelli AP: Recognition of Candida albicans by gingival fibroblasts: The role of TLR2, TLR4/CD14, and MyD88. Cytokine 106: 67-75, 2018.

12. Koc M, Siklova M, Sramkova V, Štěpán M, Krauzová E, Štich V and Rossmeislová L: Signs of deregulated gene expression are present in both CD14(+) and CD14(-) PBMC from non-obese men with family history of T2DM. Front Endocrinol (Lausanne) 11: 582732, 2021.
13. Staller S, Lindsay AK, Ramos ED, Thomas P and Srinivasan M: Changes in salivary microbial sensing proteins CD14 and TLR2 with aging. Clin Oral Investig 24: 2523-2528, 2020.
14. Aguilar-Briseno JA, Upasani V, Ellen BMT, Moser J, Pauzuolis M, Ruiz-Silva M, Heng S, Laurent D, Choeung R, Dussart P, *et al*: TLR2 on blood monocytes senses dengue virus infection and its expression correlates with disease pathogenesis. Nat Commun 11: 3177, 2020.
15. Reinhardt C: The gut microbiota as an influencing factor of arterial thrombosis. Hamostaseologie 39: 173-179, 2019.
16. Yao M, Fang C, Wang Z, Guo T, Wu D, Ma J, Wu J and Mo J: miR-328-3p targets TLR2 to ameliorate oxygen-glucose deprivation injury and neutrophil extracellular trap formation in HUVECs via inhibition of the NF-κB signaling pathway. PLoS One 19: e299382, 2024.
17. Wang Z, Fang C, Yao M, Wu D, Chen M, Guo T and Mo J: Research progress of NF-kappaB signaling pathway and thrombosis. Front Immunol 14: 1257988, 2023.
18. Griffin G: Establishing a Three Rs programme at the Canadian Council on Animal Care. Altern Lab Anim 37 (Suppl 2): S63-S67, 2009.
19. X Z: Establishment of a new animal model of traumatic limb deep vein thrombosis and related studies, 2004.
20. Jeong JJ, Woo JY, Kim KA, Han MJ and Kim DH: Lactobacillus pentosus var. plantarum C29 ameliorates age-dependent memory impairment in Fischer 344 rats. Lett Appl Microbiol 60: 307-314, 2015.
21. Lee SJ, Baek SE, Jang MA and Kim CD: SIRT1 inhibits monocyte adhesion to the vascular endothelium by suppressing Mac-1 expression on monocytes. Exp Mol Med 51: 1-12, 2019.
22. Liao X, He J, Wang R, Zhang J, Wei S, Xiao Y, Zhou Q, Zheng X, Zhu Z, Zheng Z, *et al*: TLR-2 agonist Pam3CSK4 has no therapeutic effect on visceral leishmaniasis in BALB/c mice and may enhance the pathogenesis of the disease. Immunobiology 228: 152725, 2023.
23. Mo J, Zheng T, Lei L, Dai P, Liu J, He H, Shi J, Chen X, Guo T, Yuan B and Ji G: MicroRNA-1253 suppresses cell proliferation migration and invasion of osteosarcoma by targeting MMP9. Technol Cancer Res Treat 20: 1533033821995278, 2021.
24. Yu J, Jin Y, Xu C, Fang C, Zhang Z, Chen L and Xu G: Downregulation of miR-125a-5p promotes endothelial progenitor cell migration and angiogenesis and alleviates deep vein thrombosis in mice via upregulation of MCL-1. Mol Biotechnol 65: 1664-1678, 2023.
25. Sykora D, Firth C, Girardo M, Bhatt S, Tseng A, Chamberlain A, Liedl D, Wennberg P and Shamoun FE: Peripheral artery disease and the risk of venous thromboembolism. VASA 51: 365-371, 2022.
26. Zhou M, Zhang T, Zhang B, Zhang X, Gao S, Zhang T, Li S, Cai X and Lin Y: A DNA nanostructure-based neuroprotectant against neuronal apoptosis via inhibiting toll-like receptor 2 signaling pathway in acute ischemic stroke. ACS Nano 16: 1456-1470, 2022.
27. Won Y, Yang JI, Park S and Chun JS: Lipopolysaccharide binding protein and CD14, cofactors of toll-like receptors, are essential for low-grade inflammation-induced exacerbation of cartilage damage in mouse models of posttraumatic osteoarthritis. Arthritis Rheumatol 73: 1451-1460, 2021.
28. Porta C, Consonni FM, Morlacchi S, Sangaletti S, Bleve A, Totaro MG, Larghi P, Rimoldi M, Tripodo C, Strauss L, *et al*: Tumor-Derived Prostaglandin E2 Promotes p50 NF-κB-Dependent differentiation of monocytic MDSCs. Cancer Res 80: 2874-2888, 2020.
29. Hojo K, Tamai R, Kobayashi-Sakamoto M and Kiyoura Y: Etidronate down-regulates Toll-like receptor (TLR) 2 ligand-induced proinflammatory cytokine production by inhibiting NF-κB activation. Pharmacol Rep 69: 773-778, 2017.
30. Makni L, Zidi S, Barbiroud M, Ahmed AB, Gazouani E, Mezlini A, Stayoussef M and Yacoubi-Loueslati B: Increased risks between TLR2 (-196 to -174 ins/del) and TLR3 1377C>T variants and head and neck cancers in Tunisia. Cent Eur J Immunol 44: 144-149, 2019.
31. Bishayi B, Bandyopadhyay D, Majhi A and Adhikary R: Effect of exogenous MCP-1 on TLR-2 neutralized murine macrophages and possible mechanisms of CCR-2/TLR-2 and MCP-1 signalling during Staphylococcus aureus infection. Immunobiology 220: 350-362, 2015.
32. Li S, Yang Z, Tian H, Ren S, Zhang W and Wang A: Effects of dietary carbohydrate/lipid ratios on non-specific immune responses, antioxidant capacity, hepatopancreas and intestines histology, and expression of TLR-MAPK/NF-κB signaling pathway-related genes of Procambarus clarkii. Fish Shellfish Immunol 124: 219-229, 2022.
33. Song R, Ao L, Zhao KS, Zheng D, Venardos N, Fullerton DA and Meng X: Soluble biglycan induces the production of ICAM-1 and MCP-1 in human aortic valve interstitial cells through TLR2/4 and the ERK1/2 pathway. Inflamm Res 63: 703-710, 2014.
34. Zheng X, Liu H, Ma M, Ji J, Zhu F and Sun L: Anti-thrombotic activity of phenolic acids obtained from Salvia miltiorrhiza f. alba in TNF-α-stimulated endothelial cells via the NF-κB/JNK/p38 MAPK signaling pathway. Arch Pharm Res 44: 427-438, 2021.